Available online at www.sciencedirect.com
SCIENCE DIRECT
Journal of Photochemistry and Photobiology A: Chemistry 178 (2006) 41–49
Journal of Photochemistry and Photobiology A:Chemistry
www.elsevier.com/locate/jphotochem

Effects of halogen substitution on the photochemical properties of hypericin

Rita C. Guedes [a,b,*], Leif A. Eriksson [a]

[a] *Department of Natural Sciences and Örebro Life Science Center, Örebro University, Fakultetsgatan 1, 70182 Örebro, Sweden*
[b] *Mathematical Physics Group of the University of Lisbon, Av. Prof. Gama Pinto 2, 1649-003 Lisbon, Portugal*

Received 11 February 2005; received in revised form 18 June 2005; accepted 23 June 2005
Available online 1 September 2005

Abstract

Hypericin (hyp) displays photodynamic activity under the influence of visible light, which has opened up new possibilities of utilizing hypericin derivatives as potential photodynamic therapy agents. In the current work, the effects of halogen substitution were considered through a detailed computational study of bromine, chlorine, and fluorine substitution on the geometrical structure, and electronic and phototoxic properties of the hypericin molecule by the use of density functional theory, integral equation formalism polarized continuum models, and a time-dependent formalism (TD-DFT) to the study of singlet and triplet excited states. It is concluded that the effect of halogen substitution is primarily an increase of the electron affinities and thereby increased quantum efficiency of superoxide formation of importance in photodynamic therapy.

Keywords: Hypericin; TD-DFT; Excitation energies; Phototoxicity; Halogen substitution

1. Introduction

Hypericin (hyp), a polycyclic aromatic molecule belonging to the phenantroperylene quinone family, is a natural photoactive pigment identified in both plant and animal kingdoms. It is unequivocal that the photodynamic activity displayed by hypericin under the influence of light could be used for therapy [1]. The photodynamic action of hypericin has been attributed either to the sensitized formation of singlet oxygen/superoxide anion, or to an acidification of the molecule by light-induced deprotonation. During the last decade, an increasing interest in hypericin has emerged from the discovery that the molecule has potential phototoxic antiviral and anticancer activity [2,3].

The mechanisms of excited-state photosensitization by a given molecule can be classified into two types of processes, types I and II (Fig. 1). In oxygen-dependent type I processes, the molecule is excited from the ground state to the first excited singlet state, from which it can be converted to the first triplet state by intersystem crossing. The photosensitizer triplet state is subsequently reduced by an electron donor, followed by electron transfer to molecular oxygen which generates reactive superoxide anion radicals. In oxygen-dependent type II processes, on the other hand, the excitation energy is transferred from the triplet state of the photosensitizer to molecular oxygen, generating singlet oxygen and regenerating the sensitizer in its ground state [3,4].

Hypericin has properties that makes it very promising for photodynamic therapy (PDT), such as strong absorption at long wavelengths, minimal dark toxicity, much higher clearance rate from the host body than hematoporphyrins (presently employed in PDT), and potent phototoxicity on tumours [2,5]. It has been shown that hypericin, in certain regimes of light and drug dosage, can induce apoptosis and/or necrosis [6,7].

The efficiency of hypericin for use in photodynamic therapy might be improved in two main directions [8]. First, it might be desirable to increase the quantum efficiency of the

* Corresponding author.
E-mail address: rita.guedes@nat.oru.se (R.C. Guedes).

1010-6030/$ – see front matter © 2005 Published by Elsevier B.V.
doi:10.1016/j.jphotochem.2005.06.018

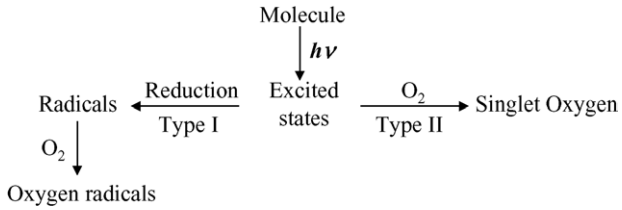

Fig. 1. Scheme of the photosensitization processes.

singlet oxygen/superoxide radical formation, and secondly, shift the main absorption band of hypericin to even longer wavelengths in order to avoid the absorptions being obscured by heme proteins. It is thought that, as a prerequisite, derivatives of this kind should retain the main functional groups of hypericin, and that the synthetic efforts could be limited to substitution outside the aromatic core. The first goal could be reached by heavy-atom substitution of the aromatic protons of hypericin as it is known that these would enhance intersystem crossing and concomitantly also enhance, to a certain degree, singlet oxygen sensitization. The second could be attained by either substituting the aromatic protons by extended conjugated substituents or by enlarging conjugation via the methyl groups [8].

Experimentally, hypericin can be stepwise bromated by adding appropriate amounts of a bromine solution in pyridine to a solution of hypericin in pyridine, followed by conventional work-up [9]. Previous work has shown that bromohypericins are potent photoactive antiviral agents [10], particularly against herpes simplex and influenza viruses. Delaey et al. have compared, in vivo, the PDT efficacy, the singlet oxygen yield, and plasma binding profile of hypericin and tetrabromohypericin [11]. As expected, the quantum yield of the bromo-derivative was enhanced, compared with hypericin, as a result of the enhanced intersystem crossing between hypericin singlet and triplet states, facilitated by the heavy-atom substitution.

Wills et al. measured the cytotoxicity, the capacity to associate with tumour cells, and the singlet oxygen yield of seven substituted hypericins, but could not correlate the changes in structure with biological activity. They suggest that more work is needed to better understand the mechanisms of hypericin analogue cytotoxicity [12]. It has also been suggested, in previous work, that minor changes in substituents would result in dramatic differences in hypericin antiviral activity [3,13].

Other studies on the substitution of hypericin have been realised with the aim of optimising properties suitable for photodynamic therapy. Obermüller et al. conducted electrophilic iodations and extended the conjugation of the hypericin molecule by attaching styryl moieties to its methyl groups [8], English et al. studied the excited-state photophysics of methylated analogues (hexamethoxyhypericin) [14], and Rahimipour et al. studied the electron transfer properties of the dibromo-, hexaacetyl-, hexamethyl-, and desmethylhypericin [15].

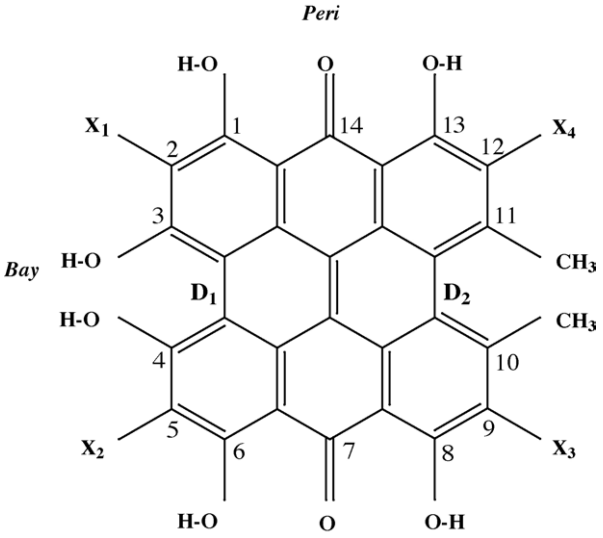

Fig. 2. Scheme of hypericin substitutions with X = Br, Cl, and F. The dihedral angles D_1 and D_2 are defined as the torsional angles of the bay and methyl group regions, respectively.

Theoretical-chemical methodology has emerged as an important complement to experimental techniques, in order to unveil properties of biochemical systems. However, to the best of our knowledge, no previous theoretical investigation has been made to explore the photochemical and photophysical properties of substituted hypericin, with the aim to optimise their use in photodynamic therapy.

In the present study, the geometrical structures, stabilities, and electronic and phototoxic properties of 12 halogenated hypericins (see Fig. 2), some of which have already proven to display potential phototoxic activity [10,11], were explored using quantum chemical methods. Throughout, the results are compared with similar experimental and theoretical data for the hypericin molecule [4].

2. Theoretical approach

All structures were optimised without symmetry constraints using Becke's three-parameter hybrid functional method [16] (B3LYP) in conjunction with the 3-21G(d) [17] and 6-31G(d) [18] basis sets. The large size of the studied molecules (54 atoms and more than 260 electrons) imposes constrains as to how large basis sets that are manageable in the quantum chemical computations, and thus the harmonic vibrational frequency analyses were performed at the lower level of theory only. All geometries were found to be minima on the respective potential energy surfaces. Data used for estimation of ionisation potentials (IPs), electron affinities (EAs), and excitation energies were calculated at the B3LYP/6-31G+(d,p)//B3LYP/6-31G(d) level of theory. In the calculation of the adiabatic EA and IP, the geometries of the neutral and the charged molecules were fully optimised, whereas for the vertical EA and IP, only the neutral

molecules were optimised and the energies of the charged species calculated on these geometries.

Vertical excitation energies, transition intensities, and oscillator strengths were computed employing time-dependent [19] density functional theory (TD-DFT) [20,21] at the B3LYP/6-31+G(d,p) level and using the optimised ground-state geometries. The use of diffuse functions has previously been shown to be critical for accurate determination of the energetics, particularly for anionic and excited states [22]. It should be emphasized, however, that the suitability of the commonly employed functionals such as B3LYP has been debated in cases of CT excitations. Dreuw and Head-Gordon attributed the possible errors of the standard exchange-correlation functionals to the so-called self interaction correction [23], and Gritsenko and Baerends showed that in the case of CT excitations, the properties of the LUMO are best described in terms of the electron affinity of the acceptor region [24]. In cases where the CT component is small, TD-DFT in combination with the B3LYP hybrid functional and the 6-31+G(d,p) basis set has previously been shown to provide excitation energies to within ∼0.2 eV (5 kcal/mol) for normal excitations[25], whereas for CT excitations, the error is about twice this size (up to ca. 0.4 eV).

Solvent effects were in the current study included through single-point calculations using the integral equation formalism of the polarised continuum model (IEF-PCM) [26,27] of Tomasi and co-workers. Two different values were used for the dielectric constant, $\varepsilon = 4.34$ and 78.39, corresponding to a hydrophobic environment and to bulk water, respectively. Previous work has shown that in the current implementation of the theoretical formalism bulk solvation effects are negligible in excitation energy calculations, and were thus neglected in order to reduce computational time. All calculations were performed using the Gaussian 03 programme [28].

3. Results and discussion

3.1. Structure and energetics

Geometry optimisations of 2-bromohypericin (1Br), 2,5-dibromohypericin (2Br), 2,5,9-tribromohypericin (3Br), 2,5,9,12-tetrabromohypericin (4Br) *with* and *without* (1Br*, 2Br*, 3Br*, and 4Br*) a bay region H-bond, as well as 2-chlorohypericin (1Cl), 2,5-dichlorohypericin (2Cl), 2-fluorohypericin (1F), and 2,5-difluorohypericin (2F), clearly demonstrate that the hypericin core structure is not influenced by the substituents (see Table 1). Due to a lack of sufficiently accurate basis sets for iodine, no iodo compounds were considered in the current work (albeit available experimentally), in order to maintain consistency.

For the bromo-substituted hypericins *without* a bay H-bond, we see that the peri O–H distances (C_1O–H and $C_{13}O$–H) remain unchanged compared with non-substituted hypericin [4]. The remaining distances are in general reduced by 0.01–0.02 Å, with the exception of the bay O–H bond distances that are marginally increased (C_3O–H = 0.98 Å and C_4O–H = 0.97–0.98 Å, comparing with 0.97 Å in hypericin [4]). The C–Br bond distances, 1.91 Å, are unaffected by the number of substituents. The torsional deformation of the hypericin skeleton increases with increasing number of bromines (D_1 = 29.9°, 30.1°, and 30.1° and D_2 = 32.6°, 32.7°,

Table 1
Structural parameters of substituted hypericins

	Bromo								Chloro		Fluoro	
	Without bay H-bond				With bay H-bond				1Cl	2Cl	1F	2F
	1Br*	2Br*	3Br*	4Br*	1Br	2Br	3Br	4Br				
Distances												
$C_1O\cdots OC_{14}$	2.53	2.54	2.54	2.54	2.52	2.52	2.53	2.52	2.52	2.52	2.54	2.54
C_1O–H	1.00	1.00	1.00	1.00	1.00	1.00	1.00	1.00	1.00	1.00	1.00	1.00
$C_1OH\cdots OC_{14}$	1.62	1.62	1.63	1.63	1.61	1.61	1.62	1.62	1.61	1.61	1.63	1.63
$C_{14}O\cdots HOC_{13}$	1.66	1.66	1.64	1.64	1.66	1.67	1.63	1.64	1.66	1.67	1.66	1.66
$C_{13}O$–H	1.00	1.00	1.00	1.00	1.00	1.00	1.00	1.00	1.00	1.00	1.00	1.00
$C_{14}O\cdots OC_{13}$	2.56	2.56	2.54	2.54	2.56	2.56	2.54	2.54	2.56	2.56	2.56	2.56
C_3–O	1.34	1.34	1.34	1.34	1.36	1.37	1.34	1.36	1.37	1.37	1.37	1.37
C_3O–H	0.98	0.98	0.98	0.98	0.98	0.98	0.98	0.98	0.98	0.98	0.98	0.98
C_4–O	1.35	1.34	1.34	1.34	1.35	1.34	1.36	1.34	1.35	1.34	1.35	1.35
C_4O–H	0.97	0.98	0.98	0.98	0.98	0.98	0.98	0.98	0.98	0.98	0.98	0.98
H···O (bay)	–	–	–	–	1.66	1.65	1.64	1.65	1.67	1.65	1.66	1.65
C_2–X_1	1.91	1.91	1.91	1.91	1.91	1.91	1.90	1.90	1.75	1.75	1.36	1.36
C_5–X_2	–	1.91	1.91	1.91	–	1.90	1.89	1.89	–	1.74	–	1.34
C_9–X_3	–		1.91	1.90	–		1.90	1.90	–	–	–	
C_{12}–X_4	–			1.90	–		–	1.90	–	–	–	
Dihedral angles												
D_1	29.9	30.1	30.1	28.2	25.9	26.6	26.6	26.6	26.2	27.1	24.5	24.3
D_2	32.6	32.7	32.8	31.0	32.9	33.0	33.1	33.5	32.9	33.0	32.9	33.0

Distances in angstroms and dihedrals in degrees.

and 32.8°); only the compound with four bromines shows a somewhat smaller distortion ($D_1 = 28.2°$ and $D_2 = 31.0°$) compared to the hypericin molecule without bay H-bond ($D_1 = 29.8°$ and $D_2 = 32.8°$) [4]. We conclude that the substitution with bromine leads to insignificant changes in the structure of the hypericin skeleton.

In bromo-substituted hypericins *with* a bay H-bond, the peri O–H distances (C_1O–H and $C_{13}O$–H) again remain unchanged compared to hypericin [4]. The remaining distances are slightly changed. Distances $C_1O\cdots OC_{14}$, $C_1OH\cdots OC_{14}$, and C_4–O decrease between 0.01 and 0.04 Å and the O–H distance C_3O–H increases by 0.01 Å. The distances $C_{14}O\cdots HOC_{13}$, $C_{14}O\cdots OC_{13}$, and C_3–O show a more irregular behaviour due to the bromo-substitution, albeit the changes are also here very small. The distances between carbon and bromine vary between 1.89 and 1.91 Å, depending on the number of bromines added. The torsional deformation of the hypericin skeleton increases with increasing number of bromines ($D_1 = 25.9°$, 26.6°, 26.6°, and 26.6° and $D_2 = 32.9°$, 33.0°, 33.1°, and 33.5°). Compared to the bay H-bond conformer of the hypericin molecule ($D_1 = 25.8°$ and $D_2 = 33.0°$) [4], the substitution in general leads to a slightly increased distortion.

In chloro-substituted hypericins, the differences in the structure between the mono- and di-substituted species are negligible. Only the bay H-bond distance decreases, from 1.67 to 1.65 Å. The distorsion of the skeleton (D_1) increases with the increasing chlorine substitution, although the dihedral D_2 remains almost unaltered.

The fluoro-substituted hypericin structures are also very similar. They show a smaller torsional deformation, $D_1 = 24.5°$ and 24.3°, due to a stronger H-bond formed in the bay region between the free bay-hydrogen and the halogen. In conclusion, the geometrical features of the substituted hypericins are all very similar to hypericin, with only small variations. No experimental parameters were found for comparison.

3.2. Formation of excited states

The photosensitizer reactions are initiated by excitation to the first excited singlet state (S_1) and intersystem crossing to the first excited triplet state (T_1) of the molecule. Our ab initio calculations showed that the lowest excited state is a $\pi \rightarrow \pi^*$ state, although the value is not in a very good agreement with the experimental result available for 2Br, 3Br, and 4Br. For example, for 2Br, the calculations give the lowest-lying excitations at 561, 482, and 435 nm, whereas the experimental data are 593, 549, and 485 nm [9]. This difference in excitation energy can be caused by two different effects: (i) spin–orbit coupling or (ii) charge transfer influence on the excitation.

Spin–orbit coupling arises from an interaction between the electron spin magnetic moment and the orbital angular momentum of the electron, and results in a mixture of different spin multiplets that gives rise to a small splitting of the spectral lines. These are in general neglected in TD-DFT calculations. In an earlier study on the similar but smaller bromobenzene, Rasmusson and co-workers showed that despite the presence of spin coupling between the lowest excited state and a repulsive $n \rightarrow \sigma^*$ triplet state, the molecule only possessed a moderate spin–orbit coupling [29–31]. In hypericin, with its considerably large aromatic ring-system, the π–π^* region will be more dominant, and hence the influence of spin–orbit interactions strongly reduced.

In terms of CT excitations, the error introduced could be in the 0.3–0.4 eV (7–10 kcal/mol) range. Comparing the theoretical and experimental numbers listed in Table 2, it appears that there is either a blue-shift in the computed data of at most 60 nm, or that the lowest-lying peak (593 nm) is simply not observed theoretically. At wavelengths around 5–600 nm, a $\Delta\lambda$ of 30 nm (the lowest transition) corresponds to a difference in excitation energy of ca. 0.1 eV, or 2.5 kcal/mol, and $\Delta\lambda = 60$ nm (the second transition) corresponds to a difference of ca. 7 kcal/mol. Considering these energetic aspects, we believe that the computational data can provide valuable insight into the fundamental properties of these compounds.

In Tables 2 and 3, we report the calculated TD-B3LYP/6-31+G(d,p)//B3LYP/6-31G(d) singlet and triplet excitation energies and oscillator strengths for the substituted hypericins. The calculated data are compared with experimental data [9], when available. Since the $S_0 \rightarrow T_n$ transitions are spin-forbidden, the probabilities (oscillator strengths) for these transitions are all zero.

3.2.1. Singlet excited states

The first singlet excited state corresponds to the $\pi \rightarrow \pi^*$ transition (HOMO–LUMO). The hypericin singlet excitation energies (Table 2) generally decrease slightly due to the halogen substitution (see Fig. 3).

Falk and Schmitzberger observed this red-shift experimentally for bromated hypericin [9]. In their work, they found

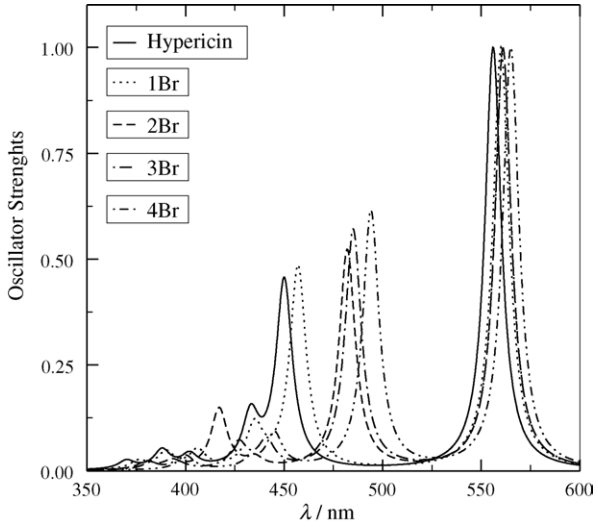

Fig. 3. Calculated absorption spectra of bromo-substituted hypericin.

Table 2
Singlet excitations energies (eV), wavelengths (nm), and oscillator strengths of the bay H-bonded substituted hypericins computed at the TD-B3LYP/6-31+G(d,p)//B3LYP/6-31G(d) level

Singlet excited states						
Hyp[a]						
E_{0-0}	2.23	2.76	2.86	3.08	3.19	3.35
λ	556	450	433	402	388	370
f	0.24	0.17	0.05	0.02	0.02	0.01
E_{0-0exp}	*2.48–2.07*[b]	*2.92–2.56*[b]				
λ_{exp}	*500–600*[b]	*425–485*[b]				
1Br						
E_{0-0}	2.21 (2.24)	2.71 (2.78)	2.85 (2.87)	3.05 (3.11)	3.18 (3.17)	3.30 (3.22)
λ	560 (553)	457 (446)	435 (432)	406 (398)	390 (391)	376 (385)
f	0.25 (0.27)	0.18 (0.22)	0.04 (0.00)	0.02 (0.01)	0.02 (0.02)	0.01 (0.00)
2Br[c]						
E_{0-0}	2.21 (2.24)	2.57 (2.72)	2.85 (2.87)	2.98 (3.09)	3.16 (3.13)	3.26 (3.16)
λ	561 (554)	482 (455)	435 (432)	417 (401)	393 (396)	380 (393)
f	0.27 (0.28)	0.19 (0.23)	0.01 (0.00)	0.07 (0.02)	0.01 (0.00)	0.01 (0.01)
E_{0-0exp}	*2.09*[d]	*2.26*[d]	*2.56*[d]	*3.17*[d]	*3.73*[d]	*4.28*[d]
λ_{exp}	*593*[d]	*549*[d]	*485*[d]	*391*[d]	*332*[d]	*290*[d]
3Br						
E_{0-0}	2.21 (2.23)	2.56 (2.67)	2.81 (2.86)	2.90 (3.03)	3.13 (3.10)	3.24 (3.13)
λ	561 (556)	485 (464)	441 (433)	427 (409)	396 (400)	382 (396)
f	0.29 (0.30)	0.22 (0.25)	0.03 (0.00)	0.03 (0.00)	0.01 (0.00)	0.01 (0.02)
E_{0-0exp}	*2.09*[d]	*2.25*[d]	*2.56*[d]	*3.17*[d]	*3.73*[d]	*4.28*[d]
λ_{exp}	*594*[d]	*550*[d]	*485*[d]	*391*[d]	*332*[d]	*290*[d]
4Br						
E_{0-0}	2.19 (2.23)	2.51 (2.62)	2.79 (2.85)	2.87 (2.97)	3.10 (3.07)	3.16 (3.11)
λ	565 (557)	494 (472)	445 (435)	433 (417)	400 (404)	392 (399)
f	0.30 (0.31)	0.24 (0.27)	0.04 (0.00)	0.01 (0.00)	0.02 (0.00)	0.00 (0.02)
E_{0-0exp}	*2.08*[d]	*2.25*[d]	*2.56*[d]	*3.16*[d]	*3.73*[d]	*4.28*[d]
λ_{exp}	*595*[d]	*550*[d]	*484*[d]	*392*[d]	*332*[d]	*290*[d]
1Cl						
E_{0-0}	2.22	2.72	2.85	3.06	3.18	3.31
λ	560	456	435	405	390	374
f	0.25	0.18	0.04	0.02	0.02	0.01
2Cl						
E_{0-0}	2.22	2.61	2.86	3.00	3.16	3.28
λ	559	475	434	413	392	378
f	0.26	0.20	0.01	0.05	0.01	0.01
1F						
E_{0-0}	2.23	2.72	2.86	3.07	3.19	3.33
λ	557	455	433	403	389	372
f	0.24	0.18	0.04	0.01	0.02	0.02
2F						
E_{0-0}	2.25	2.66	2.89	3.04	3.17	3.32
λ	551	467	429	407	392	374
f	0.24	0.20	0.01	0.04	0.01	0.01

Data for non-H-bonded hypericins are given in parenthesis.
[a] Ref. [4].
[b] Ref. [37]—the first UV transition band contains three vibronic levels, at 591, 547, and 510 nm.
[c] For 2Br, we have calculated 10 more singlet excited states (359, 350, 344, 334, 332, 323, 320, 316, 314, and 309 nm; see Fig. 4).
[d] Ref. [9].

that the absorption spectra of 2Br, 3Br, and 4Br were shifted by 4, 5, and 6 nm, respectively, compared to those of hypericin. Very similar shifts were found in the current study: 4, 5, 5, and 9 nm for 1Br, 2Br, 3Br, and 4Br, respectively. The shift relative to hypericin increases slightly with each consecutive substitution. Compared with the experimental data for 2Br, 3Br, and 4Br, our spectra are shifted to slightly shorter wavelengths, corresponding to overestimated excitation energies by ca. 0.2 eV (5 kcal/mol; see Fig. 4). We cannot exclude the possibility that a better estimate could be obtained with a larger basis set or, as mentioned above, a more sophisticated (and computationally more costly) exchange-correlation

Table 3
Triplet excitations energies (eV) and wavelengths (nm) of the bay H-bonded substituted hypericins computed at the TD-B3LYP/6-31+G(d,p)//B3LYP/6-31G(d) level

Triplet excited states						
Hyp[a]						
E_{0-0}	1.62	2.03	2.26	2.53	2.76	2.97
λ	765	611	548	491	449	418
λ_{exp}	*755*[b], *752*[c]					
1Br						
E_{0-0}	1.61 (1.63)	2.00 (2.04)	2.26 (2.28)	2.52 (2.51)	2.74 (2.81)	2.91 (2.87)
λ	769 (762)	619 (607)	549 (543)	492 (495)	453 (442)	426 (432)
2Br						
E_{0-0}	1.62 (1.63)	1.94 (2.01)	2.27 (2.28)	2.49 (2.50)	2.59 (2.76)	2.90 (2.80)
λ	767 (760)	640 (616)	546 (543)	498 (496)	478 (448)	428 (443)
3Br						
E_{0-0}	1.62 (1.63)	1.91 (1.98)	2.27 (2.28)	2.45 (2.48)	2.55 (2.70)	2.88 (2.76)
λ	763 (760)	650 (627)	546 (543)	505 (500)	487 (459)	430 (449)
4Br						
E_{0-0}	1.62 (1.63)	1.87 (1.94)	2.27 (2.28)	2.43 (2.46)	2.52 (2.68)	2.75 (2.69)
λ	765 (759)	663 (639)	547 (543)	510 (504)	491 (463)	451 (461)
1Cl						
E_{0-0}	1.61	2.00	2.26	2.52	2.74	2.92
λ	768	619	549	492	452	425
2Cl						
E_{0-0}	1.62	1.94	2.27	2.50	2.62	2.91
λ	764	628	544	496	473	427
1F						
E_{0-0}	1.63	2.00	2.27	2.53	2.75	2.93
λ	762	620	547	491	451	424
2F						
E_{0-0}	1.65	1.95	2.30	2.52	2.66	2.92
λ	752	637	538	492	466	424

Data for the non-H-bonded hypericins are given in parenthesis.
[a] Ref. [4].
[b] Ref. [38].
[c] Ref. [39].

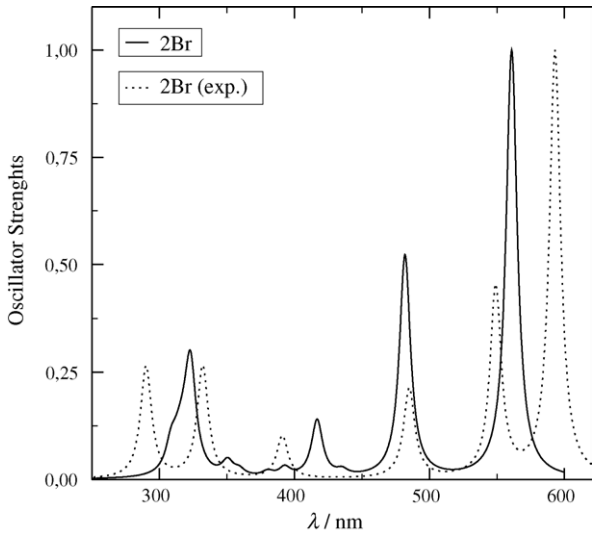

Fig. 4. Comparison of calculated and experimental [9] absorption spectra of 2Br. Note that both spectra have been normalized individually such that the strongest peak of each has oscillator strength $f = 1$.

functional. With respect to the first of these issues, basis set requirements for DFT methods are in general less significant than for high-level ab initio methods [32].

Concerning substitutions with different types of atoms, the excitation energies generally decrease in the sequence F > Cl > Br. Between the mono- and di-chloro or mono- and di-fluoro substituents, the excitation energies and absorption wavelengths usually follow the same behaviour as for the bromine substitutions. Overall, the effects are largest for the systems with two or more substituents. For all systems, the shift with increasing substituents is particularly strong for the S_2 state.

3.2.2. Triplet excited states

The triplet excitation energies generally follow the same behaviour as the singlet states in that they decrease with increasing substitution, albeit with more irregularities than the former case (cf. Table 3). For bromine substitutions, the first excited triplet state is essentially unalterated. However, the second triplet state is always shifted to longer wavelengths and depends strongly on number of substituents. On average,

the spectral shifts due to bromation are very similar to the ones reported for the singlet states.

For chlorinated hypericin, the shift in the absorption spectra is not as pronounced as in the case of bromine, whereas for the fluoro-substituted species, the wavelengths of the first excited triplet states decrease by 3 and 13 nm (1F and 2F) while the second excited triplet states increase 9 and 26 nm (1F and 2F, respectively) compared to hypericin. The triplet absorption wavelength shifts on average increase in the sequence F < Cl < Br.

3.3. Oxygen-dependent type I reactions

Hypericin and its derivatives are considered potential photosensitizers for use in photodynamic therapy. The phototoxicity of these sensitizers most probably occurs through oxygen-dependent reactions. Oxygen-dependent type I reactions involve a direct reaction of the excited triplet state of the photosensitizer with an electron donor, to generate a sensitizer radical anion. Subsequent electron transfer from the sensitizer to molecular oxygen leads to the generation of superoxide from which hydrogen peroxide and/or hydroxyl radicals can be produced, and the sensitizer is regenerated in the ground state. In Table 4, we list the computed ground-state vertical and adiabatic electron affinities (VEA and AEA) of hypericin in different solvents, as well as the energy gain when reducing the lowest excited triplet state (VEA(T_1)).

The VEA(T_1) hence represents a measure of the ability of the photoexcited drug to extract an electron from the surroundings. When substituted hypericins are excited to the first triplet state, the vertical electron affinities (VEA(T_1)) increase by more than 1.5 eV and always lie higher than the corresponding values for the parent compound. The values increase with increasing polarity of the medium, due to the increased stabilization of the reduced species. Analysing Table 4, we can see that the increase of VEA(T_1) is also correlated to the increasing number of substitutions (for example, 1Br < 2Br < 3Br < 4Br). After reduction of the drug, electron transfer to molecular oxygen will lead to the formation of the reactive superoxide radical anion and regeneration of the substituted hypericins in the ground state, provided the oxidation potential of the reduced drug is smaller than the reduction potential of molecular oxygen.

The vertical electron affinities of the substituted hypericins are in the range between 2.27 eV (1F) and 2.63 eV (4Br) in vacuum, 3.18 eV (1F) and 3.43 eV (4Br) in hydrophobic medium, and 3.43 eV (1F) and 3.63 eV (4Br) in aqueous solution. The adiabatic electron affinities are shifted to ∼0.15 eV higher energies. This small difference reflects the extent of radical anion relaxation, which in the case of hypericin is negligible. The C–X bonds increase slightly (between 0.01 and 0.02 Å) upon reduction.

Comparing the computed adiabatic electron affinities of substituted hypericins to the ones of molecular oxygen, 0.59 eV in vacuum [33] (experimental value, 0.45 eV) [34] and 3.91 eV in aqueous solution [33], we conclude that once the reduced drug is generated, the oxidizing power of O_2 in vacuum is not sufficient to extract an electron from the drug, whereas in bulk water electron transfer from the drug to molecular oxygen is accompanied with an energy gain of between 0.15 and 0.32 eV. The data for the first triplet states of substituted hypericins indicate that these in turn in most cases will be able to quench superoxide anions (VEA(T_1) between 3.89 and 5.25 eV) to generate reduced hypericin and molecular oxygen.

3.4. Oxygen-dependent type II reactions

In type II reactions, the excitation energy is directly transferred from the triplet state of the drug to the molecular oxygen, generating the very reactive singlet oxygen and regenerating the drug in the ground state. When we compare the de-excitation energy of the substituted hypericins (1.61–1.65 eV; Table 3), with the energy needed to convert molecular oxygen to singlet oxygen (0.98 eV [35]), we conclude that the T_1 excitation energy can readily be transferred from the substituted hypericins to molecular oxygen and generate singlet molecular oxygen. This process

Table 4
Vertical and adiabatic electron affinities, VEA and AEA (eV), of the ground state of the substituted hypericins and of the lowest excited triplet state in different media at the IEF-PCM//B3LYP/6-31+G(d,p) level of theory

Medium	VEA(T_1)			VEA			AEA		
	$\varepsilon = 0$	$\varepsilon = 4.34$	$\varepsilon = 78.38$	$\varepsilon = 0$	$\varepsilon = 4.34$	$\varepsilon = 78.38$	$\varepsilon = 0$	$\varepsilon = 4.34$	$\varepsilon = 78.38$
Hyp	3.78	4.71	4.99	2.16	3.09	3.37	2.31	3.24	3.52
1Br	3.90	4.80	5.06	2.29	3.19	3.45	2.43	3.34	3.59
2Br	4.02	4.88	5.12	2.40	3.27	3.51	2.54	3.41	3.64
3Br	4.14	4.97	5.19	2.51	3.35	3.57	2.65	3.70	3.49
4Br	4.25	5.05	5.25	2.63	3.43	3.63	2.76	3.56	3.76
1Cl	3.90	4.81	5.06	2.28	3.19	3.45	2.43	3.34	3.59
2Cl	4.01	4.89	5.12	2.39	3.26	3.50	2.54	3.41	3.64
1F	3.89	4.81	5.06	2.27	3.18	3.43	2.41	3.32	3.57
2F	4.00	4.88	5.12	2.35	3.24	3.47	2.50	3.38	3.61

VEA(T_1) = VEA(S_0) + $^3E_{0-0}$.

Table 5
Vertical and adiabatic ionisation potential, VIP and AIP (eV), of the ground state of the substituted hypericins and of the lowest excited triplet state in different media at the B3LYP/6-31+G(d,p) level of theory

Medium	VIP(T_1)			VIP			AIP		
	$\varepsilon = 0$	$\varepsilon = 4.34$	$\varepsilon = 78.38$	$\varepsilon = 0$	$\varepsilon = 4.34$	$\varepsilon = 78.38$	$\varepsilon = 0$	$\varepsilon = 4.34$	$\varepsilon = 78.38$
Hyp	5.45	4.34	3.98	7.07	5.96	5.60	6.95	5.86	5.50
1Br	5.52	4.42	4.05	7.14	6.04	5.66	7.02	5.94	5.56
2Br	5.59	4.49	4.09	7.20	6.10	5.71	7.09	6.00	5.62
3Br	5.65	4.55	4.14	7.27	6.17	5.77	7.16	6.07	5.67
4Br	5.71	4.61	4.20	7.33	6.23	5.82	7.22	6.13	5.73
1Cl	5.54	4.43	4.04	7.15	6.04	5.66	7.04	5.94	5.57
2Cl	5.61	4.49	4.09	7.23	6.11	5.72	7.12	6.02	5.62
1F	5.55	4.43	4.04	7.18	6.05	5.67	7.06	5.94	5.56
2F	5.64	4.49	4.08	7.29	6.13	5.73	7.17	6.02	5.63

$VIP(T_1) = VIP(S_0) - {}^3E_{0\text{–}0}$.

will of course be in competition with the above-described reduction of the drugs.

3.5. Direct electron transfer to O_2

Another reaction that can take place upon absorbing radiation is the direct electron transfer to molecular oxygen, oxidizing the drug. The viability of this reaction, i.e., the extent of drug ionisation, can be measured by comparing the ionisation potentials of the drugs with the electron affinities of O_2. Table 5 reports the calculated data for the vertical and adiabatic ionisation potentials from the ground state, and the vertical IP from the lowest-lying triplet state of substituted hypericins in different media.

Once again, the structural relaxation of the radical cations is very small (the difference between the VIP and AIP is ∼0.10 eV), in analogy with the behaviour observed for the hypericin molecule [4]. Due to the high electronegativities of the halogens, the hypericin molecule is more easily ionised than any of the substituted species. The ionisation potentials increase with increasing number of heavy-atom substitutions of the aromatic protons in hypericin. In addition, the larger the dielectric constant of the medium, the easier it ionises the drug due to solvent stabilization of the charged species. Our results suggest that O_2 is not able to oxidize any of the substituted hypericins in the ground (or triplet) states and consequently cannot generate superoxide anion radicals by this process. These results, increased EA and IP upon halogen substitution, are in accordance with previous studies on, e.g., halouracils [36].

3.6. Auto ionisation

Once a drug is irradiated and excited to the first excited triplet state, another molecule in the ground or triplet state may be able to reduce it. Comparing the $VEA(T_1)$ and VIP of the substituted hypericin, we conclude that it is improbable that a molecule in the triplet state could be reduced by neighbouring molecule in the ground state. However, when comparing $VEA(T_1)$ with $VIP(T_1)$, our results indicate that in bulk water, but not in vacuum, two molecules in the triplet state can transfer an electron and disproportionate/auto ionise, once excited.

4. Conclusions

In the present computational study of the effects of halogen substitution on the hypericin molecule, we have explored the geometrical structures and electronic and phototoxic properties by the use of density functional theory, integral equation formalism polarized continuum model (to include solvent effects), and a time-dependent formalism to determine singlet and triplet excited states.

The results are throughout compared with a similar study of the hypericin molecule [4] and with experimental data [9] when available. We found that halogen substitutions have very small effects on the structure of hypericin. The carbon skeletons of the bromo- and chloro-substituted hypericins are slightly more twisted than in hypericin, and increase with increasing number of substituents, which may lead to somewhat altered interactions with the surroundings, whereas on the other hand, fluoro-substituted hypericins have a less twisted skeleton as a result of the stronger H-bond formed in the bay region between the free bay-hydrogen and the halogen.

The excitation energies generally decrease with increasing halogen substitution. In the case of bromo-substitution, the shift in the absorption spectra is very similar to available experimental data [9]. The shifts are in all cases very small. The de-excitation energy of all the substituted hypericins is such that these will provide a good source of singlet oxygen, albeit there will not be any observable difference in quantum yield of $^1O_2$ directly.

The inclusion of solvent effects leads to an increase of the EAs and to a reduction of the IPs of the halogen-substituted hypericins. The EAs calculated in both the gas phase and solution increase according to hyp < F < Cl ≤ Br. We propose that all the substituted hypericins are more easily reduced than the hypericin molecule. The triplet reduction potentials increase

with increasing polarity of the medium and with increasing number of substituents (for example, 1Br < 2Br < 3Br < 4Br). We propose that, once the reduced drug is generated, the oxidizing power of O_2 in vacuum is not strong enough to extract an electron there from, but probably there will be electron transfer from the drug to molecular oxygen in bulk water; hence, halogen substitution will provide an increased quantum yield of superoxide anions. The final nature of the generated reactive oxygen species will hence depend on the presence/absence of a nearby electron donor to the excited photosensitizer.

The calculated IPs increase according to hyp < Br ≤ Cl ≤ F. Our results suggest that O_2 is not able to oxidize any of the substituted hypericins in the ground (or triplet) state and consequently cannot generate superoxide anion radicals by a direct process. Auto ionisation of the substituted hypericins is only possible in bulk water, between two neighbouring drugs in the triplet state.

We thus conclude that the halogen substitution has the potential to improve the hypericin efficacy for use in PDT, primarily by increasing the quantum efficiency of superoxide radical anion formation in bulk water by way of its altered EA. The effects on the geometrical structures and on the excitation energies (singlet oxygen yield) caused by halogen substitution are on the other hand very small.

Acknowledgements

RCG thanks Fundação para a Ciência e a Tecnologia for financial support through a post-doctoral grant (SFRH/BPD/11501/2002). The Swedish Science Research Council (VR) is acknowledged for financial support (LAE). We also acknowledge grants of computing time at the supercomputing facilities in Linköping (NSC).

References

[1] H. Falk, Angew. Chem. Int. Ed. 38 (1999) 3116–3136.
[2] P. Miskovsky, Curr. Drug Targets 3 (2002) 55–84.
[3] G.A. Kraus, W. Zhang, M.J. Fehr, J.W. Petrich, Y. Wannemuehler, S. Carpenter, Chem. Rev. 96 (1996) 523–535.
[4] R.C. Guedes, L.A. Eriksson, J. Photochem. Photobiol. A: Chem. 172 (2005) 293–299.
[5] Z. Diwu, Photochem. Photobiol. 61 (1995) 529–539.
[6] A.M. Vantieghem, Z. Assefa, P. Vandenabeele, et al., FEBS Lett. 440 (1998) 19–24.
[7] G. Lavie, C. Kaplinsky, A. Toren, I. Aizman, D. Meruelo, Y. Mazur, M. Mandel, Br. J. Cancer 79 (1999) 423–432.
[8] R.A. Obermüller, K. Hohenthanner, H. Falk, Photochem. Photobiol. 74 (2001) 211–215.
[9] H. Falk, W. Schmitzberger, Monatsh. Chem. 124 (1993) 77–81.
[10] J.B. Hudson, E. Delaey, P.A. de Witte, Photochem. Photobiol. 70 (1999) 820–822.
[11] E. Delaey, I. Zupko, B. Chen, A. Derycke, F. Van Laar, D. de Vos, P.A. de Witte, Int. J. Oncol. 23 (2003) 519–524.
[12] N.J. Wills, J. Park, J. Wen, S. Kesavan, G.A. Kraus, J.W. Petrich, S. Carpenter, Photochem. Photobiol. 74 (2001) 216–220.
[13] G.A. Kraus, W. Zhang, S. Carpenter, Y. Wannemuehler, Bioorg. Med. Chem. Lett. 5 (1995) 2633–2636.
[14] D.S. English, W. Zhang, G.A. Kraus, J.W. Petrich, J. Am. Chem. Soc. 119 (1997) 2980–2986.
[15] S. Rahimipour, C. Palivan, D. Freeman, F. Barbosa, M. Fridkin, L. Weiner, Y. Mazur, G. Gescheidt, Photochem. Photobiol. 74 (2001) 149–156.
[16] A.D. Becke, J. Chem. Phys. 98 (1993) 5648.
[17] M.S. Gordon, J.S. Binkley, J.A. Pople, W.J. Pietro, W.J. Hehre, J. Am. Chem. Soc. 104 (1982) 2797.
[18] R. Ditchfield, W.J. Hehre, J.A. Pople, J. Chem. Phys. 54 (1971) 724.
[19] E. Casida, in: D.P. Chong (Ed.), Recent Advances in Density Functional Methods, Part 1, World Scientific, Singapore, 1995.
[20] R.E. Stratmann, G.E. Scuseria, M.J. Frisch, J. Chem. Phys. 109 (1998) 8218–8224.
[21] M.E. Casida, C. Jamorski, K.C. Casida, D.R. Salahub, J. Chem. Phys. 108 (1998) 4439–4449.
[22] S.D. Wetmore, L.A. Eriksson, R.J. Boyd, in: L.A. Eriksson (Ed.), Theoretical and Computational Chemistry, Theoretical Biochemistry—Processes and Properties of Biological Systems, vol. 9, Elsevier, Amsterdam, 2001.
[23] A. Dreuw, M. Head-Gordon, J. Am. Chem. Soc. 126 (2004) 4007–4016.
[24] O. Gritsenko, E.J. Baerends, J. Chem. Phys. 121 (2004) 655–660.
[25] J. Llano, L.A. Eriksson, Phys. Chem. Chem. Phys. 6 (2004) 2426.
[26] B. Menucci, R. Cammi, J. Tomasi, J. Phys. Chem. 109 (1998) 2798–2807.
[27] D.M. Chipman, J. Chem. Phys. 112 (2000) 5558–5565;
E. Cancès, B. Mennucci, J. Chem. Phys. 114 (2001) 4744–4745.
[28] M.J. Frisch, G.W. Trucks, H.B. Schlegel, G.E. Scuseria, M.A. Robb, J.R. Cheeseman, J.A. Montgomery Jr., T. Vreven, K.N. Kudin, J.C. Burant, J.M. Millam, S.S. Iyengar, J. Tomasi, V. Barone, B. Mennucci, M. Cossi, G. Scalmani, N. Rega, G.A. Petersson, H. Nakatsuji, M. Hada, M. Ehara, K. Toyota, R. Fukuda, J. Hasegawa, M. Ishida, T. Nakajima, Y. Honda, O. Kitao, H. Nakai, M. Klene, X. Li, J.E. Knox, H.P. Hratchian, J.B. Cross, C. Adamo, J. Jaramillo, R. Gomperts, R.E. Stratmann, O. Yazyev, A.J. Austin, R. Cammi, C. Pomelli, J.W. Ochterski, P.Y. Ayala, K. Morokuma, G.A. Voth, P. Salvador, J.J. Dannenberg, V.G. Zakrzewski, S. Dapprich, A.D. Daniels, M.C. Strain, O. Farkas, D.K. Malick, A.D. Rabuck, K. Raghavachari, J.B. Foresman, J.V. Ortiz, Q. Cui, A.G. Baboul, S. Clifford, J. Cioslowski, B.B. Stefanov, G. Liu, A. Liashenko, P. Piskorz, I. Komaromi, R.L. Martin, D.J. Fox, T. Keith, M.A. Al-Laham, C.Y. Peng, A. Nanayakkara, M. Challacombe, P.M.W. Gill, B. Johnson, W. Chen, M.W. Wong, C. Gonzalez, J.A. Pople, Gaussian 03, Revision A.3, Gaussian, Inc., Pittsburgh, PA, 2003.
[29] C.E. Moore, Atomic Energy Levels, Nat. Stand. Ref. Data Ser., vol. II, Nat Bur. Stand., US, 1971, p. 159.
[30] M. Rasmusson, R. Lindh, N. Lascoux, A.N. Tarnovsky, M. Kadi, O. Kühn, V. Sundström, E. Åkesson, Chem. Phys. Lett. 367 (2003) 759–766.
[31] M. Kadi, A.N. Tarnovsky, M. Rasmusson, J. Davidsson, E. Åkesson, Chem. Phys. Lett. 350 (2001) 93–98.
[32] B. Durbeej, L.A. Eriksson, Chem. Phys. Lett. 375 (2003) 30–38.
[33] J. Llano, J. Raber, L.A. Eriksson, J. Photochem. Photobiol. A: Chem. 154 (2003) 235–243.
[34] M.J. Travers, D.C. Cnowles, G.B. Ellison, Chem. Phys. Lett. 164 (1989) 449.
[35] K.P. Huber, G. Herzberg, Molecular Spectra and Molecular Structure, Part. IV. Constants of Diatomic Molecules, Van Nostrand, NY, 1979.
[36] S.D. Wetmore, R.J. Boyd, L.A. Eriksson, Chem. Phys. Lett. 343 (2001) 151.
[37] J.L. Wynn, T.M. Cotton, J. Phys. Chem. 99 (1995) 4317–4323.
[38] S.M. Arabei, J.P. Galaup, P. Jardon, Chem. Phys. Lett. 270 (1997) 31–36.
[39] A.P. Darmanyan, W.S. Jenks, D. Eloy, P. Jardon, J. Phys. Chem. B 103 (1999) 3323–3331.